

Rapid emplacement of massive Duluth Complex intrusions within the Midcontinent Rift

Nicholas L. Swanson-Hysell¹, Steven A. Hoaglund², James L. Crowley³, Mark D. Schmitz³, Yiming Zhang¹, James D. Miller Jr.²

¹ Department of Earth and Planetary Science, University of California, Berkeley, CA, USA

² Department of Earth and Environmental Sciences, University of Minnesota, Duluth, MN, USA

³ Department of Geosciences, Boise State University, Boise, ID, USA

ABSTRACT

The Duluth Complex is one of the largest mafic intrusive complexes in the world. It was emplaced as the Midcontinent Rift developed in Laurentia's interior during an interval of magmatism and extension from *ca.* 1109 to 1084 Ma. This duration of magmatic activity is more protracted than is typical for large igneous provinces interpreted to have formed from decompression melting of upwelling mantle plumes. While the overall duration of magmatic activity was protracted, there were intervals of more voluminous magmatism. New high-precision $^{206}\text{Pb}/^{238}\text{U}$ dates for the anorthositic and layered series of the Duluth Complex constrain these units to have been emplaced *ca.* 1096 Ma in less than 1 million years. Comparison of paleomagnetic data from these units with the apparent polar wander path supports this interpretation. This timing corresponds with eruptions of the North Shore Volcanic Group. The rapid emplacement of Duluth Complex intrusions and these eruptions bear similarities to the geologically short duration of well-dated large igneous provinces. These data support hypotheses that call upon the co-location of lithospheric extension and anomalously hot upwelling mantle undergoing decompression melting. This rapid magmatic pulse occurred more than 10 million years after initial magmatic activity following more than 20° of latitudinal plate motion. A likely scenario is one in which upwelling mantle encountered the base of Laurentian lithosphere and

18 flowed via “upside-down drainage” to the locally thinned lithosphere of the Midcontinent Rift.

19 INTRODUCTION

20 The Midcontinent Rift represents a protracted tectonomagmatic event in the interior of Laurentia
21 (the North American craton). Voluminous outpouring of lava and emplacement of intrusions
22 accompanied rift development (Fig. 1). Magmatic activity initiated *ca.* 1109 Ma and continued
23 until *ca.* 1084 Ma (Swanson-Hysell et al., 2019). Preserved thicknesses of the volcanic successions
24 range from nearly 10 km for partial sections exposed on land, such as along the North Shore of
25 Minnesota (Green et al., 2011), to ~25 km under Lake Superior (Cannon, 1992). These volcanics
26 and associated intrusions are much more voluminous than is typical for a tectonic rifting event.

27 Analysis of seismic data leads to an estimate that total eruptive volume exceeded $2 \times 10^6 \text{ km}^3$
28 and that a much greater volume was added to the lithosphere as intrusions and an underplate
29 (Cannon, 1992). The ~25 Myr duration of volcanism in the Midcontinent Rift is much longer
30 than is typical for large igneous province emplacement associated with decompression melting of
31 an upwelling mantle plume. Well-dated large igneous provinces, such as the Central Atlantic
32 Magmatic Province (Blackburn et al., 2013), the Karoo-Ferrar (Burgess et al., 2015), and the
33 Deccan Traps (Schoene et al., 2019; Sprain et al., 2019) have durations of <1 Myr for the bulk of
34 their magmatism. An explanation for prolonged volcanism in the Midcontinent Rift could
35 attribute rift initiation and initial volcanism via plume arrival with continued volcanism resulting
36 from rift-driven asthenospheric upwelling. However, the most voluminous period of magmatism
37 occurred more than 10 million years after initial flood volcanism during an interval known as the
38 “main magmatic stage” (Vervoort et al., 2007). Main stage magmatism has been attributed to an
39 upwelling mantle plume based both on the large volume and geochemical signatures (Nicholson
40 and Shirey, 1990; White and McKenzie, 1995).

41 Pioneering Midcontinent Rift geochronology utilized $^{207}\text{Pb}/^{206}\text{Pb}$ dates on zircon from
42 volcanics (Davis and Green, 1997) and intrusions (Paces and Miller, 1993) to illuminate the

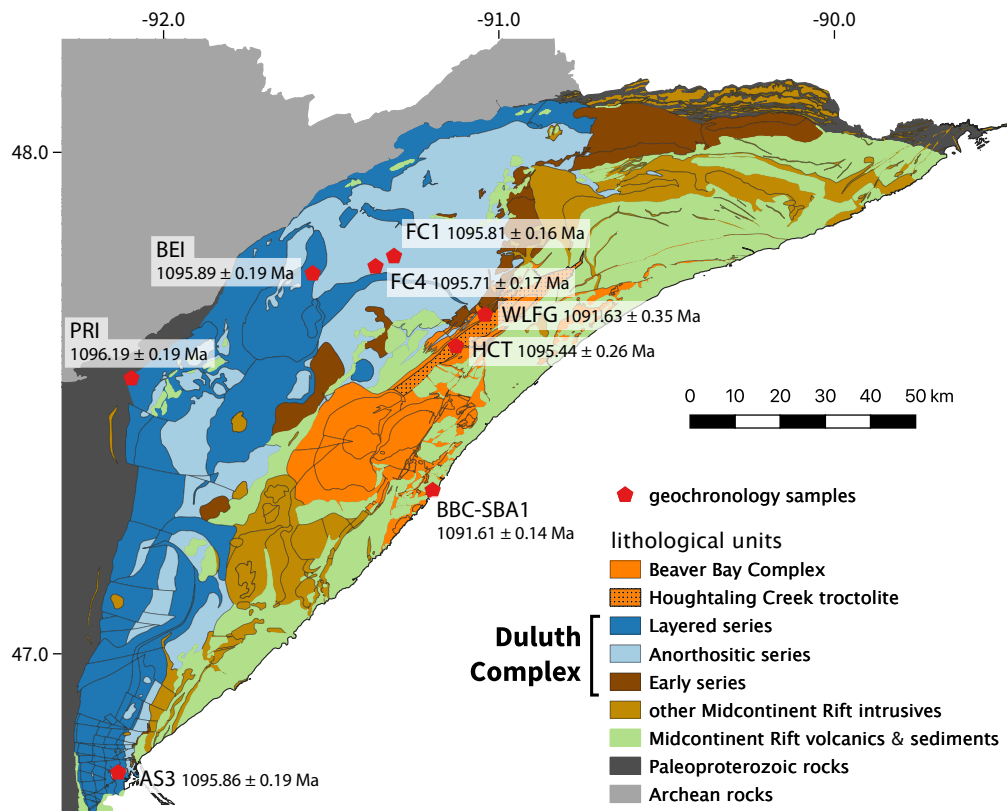


Figure 1. Geologic map of NE Minnesota (simplified from Jirsa et al., 2011) highlighting major intrusive complexes of the Midcontinent Rift and showing geochronology sample locations. U-Pb dates from the anorthositic and layered series of the Duluth Complex (shown in light and dark blue) indicate rapid emplacement in less than 1 million years.

43 magmatic history. Subsequent advances in U-Pb geochronology enable higher precision
 44 $^{206}\text{Pb}/^{238}\text{U}$ dates to be used when chemical abrasion methods have mitigated Pb-loss (Mattinson,
 45 2005). An updated chronostratigraphic framework for Midcontinent Rift volcanics was recently
 46 published (Swanson-Hysell et al., 2019) that included new U-Pb dates developed using these
 47 methods (Fig. 2). With these higher precision constraints, the timing and tempo of magmatic
 48 activity within the rift can be reevaluated. Of particular interest is whether magmatic activity
 49 was continuous or punctuated by pulses. Key to evaluating this question is the timing of
 50 emplacement of intrusive rocks throughout the Midcontinent Rift, particularly the largest
 51 intrusive suite – the Duluth Complex (Fig. 1). With its arcuate area of 5630 km^2 , the tholeiitic
 52 Duluth Complex is the second-largest exposed mafic intrusive complex on Earth (Miller et al.,

53 2002). It was emplaced as sheet-like intrusions into the base of a comagmatic volcanic succession
54 with the majority of its volume associated with the anorthositic series and the layered series of
55 gabbroic and troctolitic cumulates (Miller et al., 2002; Fig. 1). We present $^{206}\text{Pb}/^{238}\text{U}$ dates from
56 the Duluth Complex, as well as the Beaver Bay Complex, to establish the duration of Duluth
57 Complex magmatism and contextualize it with the chronology of volcanism.

58 METHODS and RESULTS

59 U-Pb geochronology methods for isotope dilution thermal ionization mass spectrometry
60 (ID-TIMS) follow Schmitz (2012). Zircon crystals were chemically abraded prior to analysis in the
61 Boise State Isotope Geology Laboratory. Weighted means were calculated from multiple single
62 zircon dates with some dates being excluded due to Pb-loss (Fig. 2 and Table 1).¹ These
63 $^{206}\text{Pb}/^{238}\text{U}$ dates can be compared to one another, and to the volcanic dates of Swanson-Hysell
64 et al. (2019), at the level of analytical uncertainty (X error in Table 1) given that they all have
65 been developed using EARTHTIME tracer solutions (Condon et al., 2015). This analytical
66 uncertainty will be referred to when dates are reported and discussed in the text.

67 The Duluth Complex anorthositic series comprises plagioclase-rich gabbroic cumulates varying
68 from anorthositic gabbro to anorthosite. Samples FC1 and FC4b are from gabbroic anorthosite
69 exposures near the former logging town of Forest Center. A weighted mean $^{206}\text{Pb}/^{238}\text{U}$ date for
70 FC1 of 1095.81 ± 0.16 Ma is calculated based on 10 single zircon dates (Table 1). The FC4b date
71 is indistinguishable from FC1 with a weighted mean $^{206}\text{Pb}/^{238}\text{U}$ date of 1095.71 ± 0.17 Ma based
72 on dates from 8 zircons. These dates are indistinguishable from the weighted mean $^{206}\text{Pb}/^{238}\text{U}$
73 date of 1095.86 ± 0.19 Ma developed from chemically-abraded zircons of gabbroic anorthosite
74 sample AS3 collected from the anorthositic series in the vicinity of Duluth (Schoene et al., 2006;

¹GSA Data Repository item 2020XXX, table of individual zircon dates is available online at <http://www.geosociety.org/datarerepository>. All paleomagnetic data and interpreted specimen directions are available to the measurement level in the MagIC database (<https://earthref.org/MagIC/doi/>). All code associated with statistical tests and data visualization is available within a Zenodo repository (currently available for reviewers in this Github repository: https://github.com/Swanson-Hysell-Group/2020_Duluth_Complex).

75 Fig. 2, Table 1).

76 The layered series of the Duluth Complex is a suite of stratiform troctolitic to gabbroic
 77 cumulates that were emplaced as discrete intrusions (Fig. 1). The PRI sample is a coarse-grained
 78 augite troctolite from the Partridge River intrusion which is at the base of the complex in contact
 79 with underlying Paleoproterozoic metasedimentary rocks (Fig. 1). Data from 6 zircons result in a
 80 weighted mean $^{206}\text{Pb}/^{238}\text{U}$ date of 1096.19 ± 0.19 Ma (Fig. 2). The BEI sample is a
 81 coarse-grained olivine gabbro from the Bald Eagle intrusion. This intrusion has been interpreted
 82 as one of the youngest layered series units based on cross-cutting relationships inferred from
 83 aeromagnetic data (Miller et al., 2002). Dates from 6 zircons of BEI result in a weighted mean
 84 $^{206}\text{Pb}/^{238}\text{U}$ date of 1095.89 ± 0.19 Ma (Fig. 2) that is indistinguishable from the anorthositic
 85 series dates.

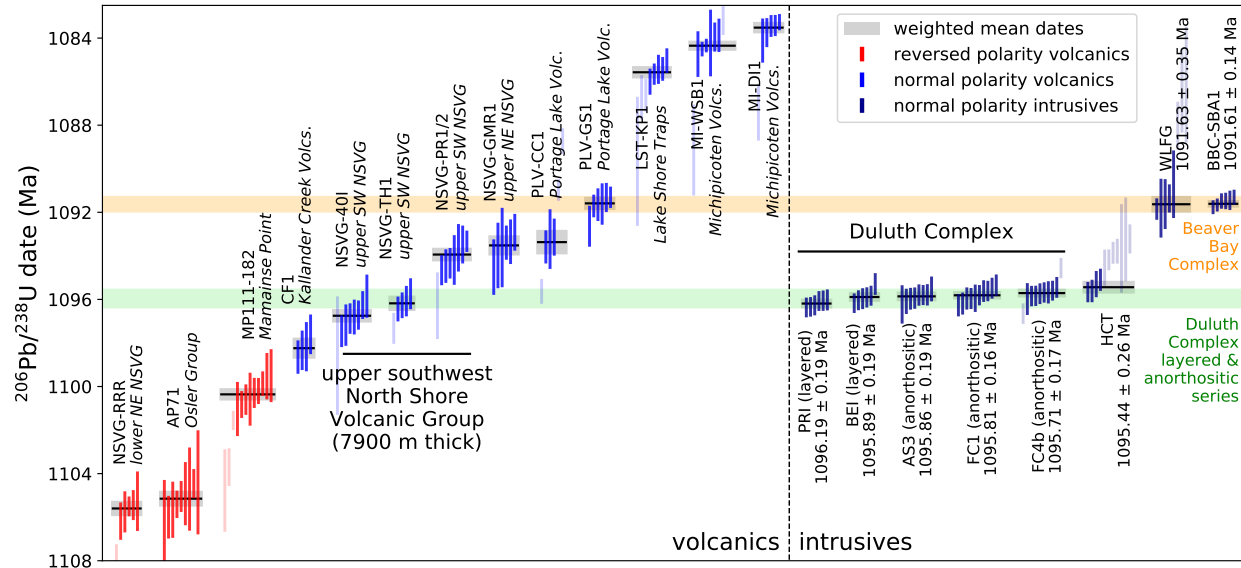


Figure 2. Date bar plot of CA-ID-TIMS $^{206}\text{Pb}/^{238}\text{U}$ dates for Midcontinent Rift volcanics and intrusives. Each vertical bar represents the date for an individual zircon while the horizontal lines and grey boxes represent the weighted means and their uncertainty.

86 The Beaver Bay complex is a suite of dominantly hypabyssal intrusions that cross-cut the
 87 North Shore Volcanic Group (Fig. 1). Sample HCT is an augite troctolite from the Houghtaling
 88 Creek troctolite. The medium-grained olivine-plagioclase cumulates of this intrusion are

89 interpreted to have been emplaced as a macrodike (Miller et al., 2001). While some zircons from
 90 HCT have Pb-loss that was not fully mitigated by chemical abrasion, dates from 4 concordant
 91 zircons result in a weighted mean $^{206}\text{Pb}/^{238}\text{U}$ date of 1095.44 ± 0.26 Ma (Fig. 2). A sample of
 92 coarse-grained ferrodiorite was collected as WLFG from the Wilson Lake ferrogabbro of the
 93 Beaver Bay Complex. This plug-shaped zoned intrusion was emplaced into the roof zone of the
 94 Duluth Complex. Dates from 5 zircons result in a weighted mean $^{206}\text{Pb}/^{238}\text{U}$ date of $1091.63 \pm$
 95 0.35 Ma (Fig. 2). This date overlaps within uncertainty with the $^{206}\text{Pb}/^{238}\text{U}$ date of $1091.61 \pm$
 96 0.14 Ma from a Silver Bay intrusion of the Beaver Bay Complex (Fairchild et al., 2017; Figs. 1
 97 and 2).

Table 1. Summary of CA-ID-TIMS $^{206}\text{Pb}/^{238}\text{U}$ dates from Midcontinent Rift intrusions

Sample	Group	Latitude Longitude	$^{206}\text{Pb}/^{238}\text{U}$ date (Ma)	Error (2σ)			MSWD	n
				X	Y	Z		
PRI <i>Partridge River intrusion</i>	Duluth Complex (layered series)	47.5480° N 92.1074° W	1096.19	0.19	0.36	1.15	0.45	6
BEI <i>Bald Eagle intrusion</i>	Duluth Complex (layered series)	47.7516° N 91.5680° W	1095.89	0.19	0.36	1.15	1.59	6
AS3 <i>Duluth anorthosite</i>	Duluth Complex (anorthositic series)	46.7621° N 92.1590° W	1095.86	0.19	0.36	1.15	0.43	8
FC1 <i>Forest Center anorthosite</i>	Duluth Complex (anorthositic series)	47.7827° N 91.3266° W	1095.81	0.16	0.34	1.14	1.44	10
FC4b <i>Forest Center anorthosite</i>	Duluth Complex (anorthositic series)	47.7677° N 91.3753° W	1095.71	0.17	0.35	1.14	0.38	8
HCT <i>Houghtaling Creek troctolite</i>	Beaver Bay Complex	47.6009° N 91.1497° W	1095.44	0.26	0.40	1.16	1.13	4
WLFG <i>Wilson Lake ferrogabbro</i>	Beaver Bay Complex	47.6620° N 91.0619° W	1091.63	0.35	0.46	1.18	0.74	5
BBC-SBA1 <i>Silver Bay aplite</i>	Beaver Bay Complex	47.6620° N 91.0619° W	1091.61	0.14	0.30	1.2	1.0	6

Notes: X—internal (analytical) uncertainty in the absence of external or systematic errors; Y—uncertainty incorporating the U-Pb tracer calibration error; Z—uncertainty including X and Y, as well as ^{238}U decay constant uncertainty (0.108%; Jaffey et al., 1971). This Z error needs to be utilized when comparing to dates developed using other decay systems (e.g., $^{40}\text{Ar}/^{39}\text{Ar}$, $^{187}\text{Re}-^{187}\text{Os}$); MSWD=mean square of weighted deviates; n=number of individual zircon dates included in the calculated sample mean date. All dates are from this study with the exceptions of AS3 which was published in Schoene et al. (2006) and BBC-SBA1 which was published in Fairchild et al. (2017). Data for individual zircons are provided in the Data Repository.

98 Paleomagnetic data from sites of the layered series (37 sites) and the anorthositic series (11
 99 sites) in the vicinity of the city of Duluth were published in Beck (1970) (Fig. 3). Statistical tests
 100 show site directions of the layered and anorthositic series to share a common mean, consistent
 101 with their overlapping U-Pb dates. In order to have paleomagnetic data directly paired with the

102 geochronology, oriented cores were collected and analyzed from the sites of the FC1, FC4 and
 103 HCT samples. Magnetization was measured on a 2G DC-SQUID magnetometer at UC Berkeley.
 104 Samples underwent alternating field or thermal demagnetization steps and fits were made using
 105 the PmagPy software (Tauxe et al., 2016). While Beck (1970) did not discuss or implement tilt
 106 corrections, the Duluth Complex and overlying lava flows gently dip towards Lake Superior and
 107 the paleomagnetic data need to be corrected for this tilt. We compile abundant igneous layering
 108 orientation measurements, which are similar to the orientations of overlying lavas and interflow
 109 sediments, and use them for tilt-correction.

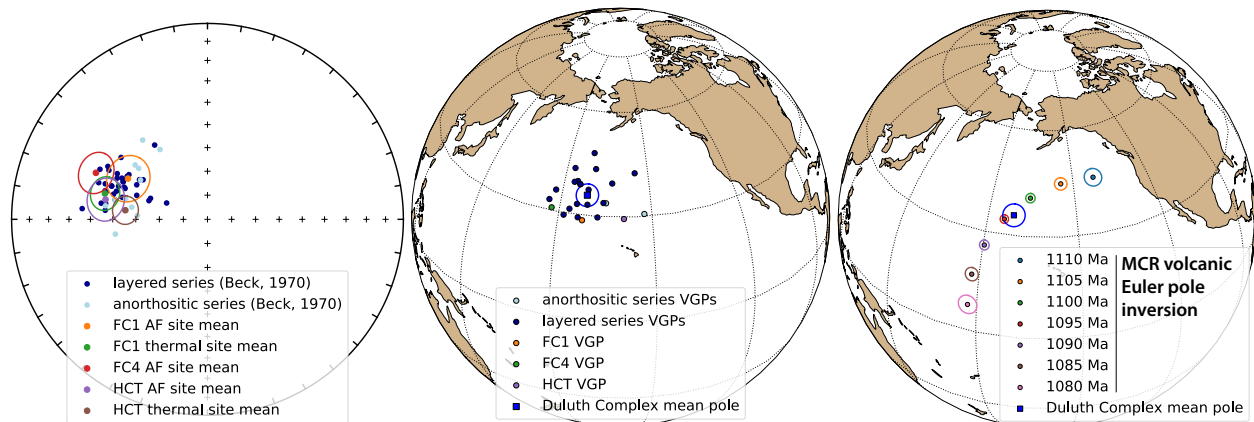


Figure 3. Left panel: tilt-corrected site mean paleomagnetic directions from anorthositic and layered series sites of Beck (1970) in the vicinity of Duluth and from the FC1, FC4, and HCT sites. Center panel: Virtual geomagnetic poles (VGPs) for sites with $\alpha_{95} < 15^\circ$ give a mean pole of: 188.7° E, 35.6° N, $N=24$, $A_{95}=3.1$, $k=92$. Right panel: Duluth Complex paleomagnetic pole shown with a synthesized pole path developed using an Euler pole inversion of Midcontinent Rift volcanic poles.

110 The rapid progression of poles within the Midcontinent Rift apparent polar wander path
 111 (APWP) enable these paleomagnetic data to give chronological insight. The positions of poles
 112 from the early stage of rift magmatism are quite different from main stage lavas (Fig. 3). The
 113 similar position of virtual geomagnetic poles (VGPs) from across the Duluth Complex layered and
 114 anorthositic series, including the FC sites, is consistent with contemporaneous emplacement and
 115 they can be combined into a mean pole (Fig. 3). This paleomagnetic pole can be compared to a
 116 synthesized Midcontinent Rift APWP developed using an Euler pole inversion of the
 117 chronostratigraphically-constrained volcanic poles (Swanson-Hysell et al., 2019). The Duluth

118 Complex pole lies between the 1100 Ma and 1095 Ma path positions with the A_{95} uncertainty of
119 the pole overlapping with the two angular standard deviations ellipse of the 1095 Ma path
120 position. This result is consistent with a *ca.* 1096 Ma age for the layered and anorthositic series
121 and strengthens the correlation with the volcanics.

122 **DISCUSSION**

123 The new U-Pb dates, together with the paleomagnetic data, imply that the bulk of both the
124 layered series and the anorthositic series of the Duluth Complex were emplaced in less than 1
125 million years. With the oldest date of 1096.19 ± 0.19 Ma and the youngest of 1095.71 ± 0.17 Ma,
126 the five dates from these series are within 500,000 years of one another and within 850,000 years if
127 the 2σ errors are considered (Fig. 2). This emplacement was coeval with eruption of the upper
128 southeast sequence of the North Shore Volcanic Group (NSVG) which comprises \sim 7900 meters of
129 lavas and is the thickest exposed Midcontinent Rift volcanic succession. The indistinguishable
130 ages of the anorthositic and layered series, together with coeval NSVG eruptions, indicate that *ca.*
131 1096 Ma there was a large pulse of melt generation.

132 The 1095.44 ± 0.26 Ma age of the Houghtaling Creek troctolite is indistinguishable from the
133 younger Duluth Complex dates. This result indicates that this pulse of voluminous magmatic
134 activity is represented in some intrusions within the Beaver Bay Complex. A younger pulse of
135 Beaver Bay Complex magmatism postdates NSVG eruptions as units such as the Beaver River
136 diabase and the Silver Bay intrusions penetrate the youngest NSVG lavas, including the 1093.94
137 ± 0.28 Ma Palisade Rhyolite (Miller et al., 2001; Swanson-Hysell et al., 2019; Fig. 1). The age of
138 this magmatism is represented by the indistinguishable dates of 1091.63 ± 0.35 Ma for the Wilson
139 Lake ferrogabbro and 1091.61 ± 0.14 Ma from the Silver Bay intrusions (Fig. 2; Table 1). This
140 younger Beaver Bay Complex magmatism is coeval with the eruption of the >5 km thick Portage
141 Lake Volcanics that are exposed on the Keweenaw Peninsula and Isle Royale (Fig. 2).

142 Rapid emplacement of the voluminous layered and anorthositic series of the Duluth Complex
143 bears similarities to the geologically short duration (<1 Myr) of well-dated continental flood
144 basalt provinces (Burgess et al., 2015; Schoene et al., 2019). This similarity supports the
145 hypothesis put forward by Green (1983), and advanced by others including Cannon and Hinze
146 (1992) and Stein et al. (2015), that the co-location of massive magmatism and rifting is the result
147 of lithospheric extension atop decompression melting of an upwelling mantle plume.
148 Contemporaneous heating of Laurentia lithosphere 600 km to the north of the rift is indicated by
149 thermochronologic data from middle to lower crustal xenoliths (Edwards and Blackburn, 2018).
150 Basaltic magma was also emplaced throughout the Southwest large igneous province coeval with
151 rift magmatism, including sills more than 2300 km from Duluth (Bright et al., 2014). That such a
152 broad region of Laurentia lithosphere experienced heating and magmatism supports the
153 hypothesized large-scale mantle upwelling.

154 Both the *ca.* 1108 early stage and *ca.* 1096 Ma main stage volcanism within the Midcontinent
155 Rift was voluminous and interpreted to be the result of a plume-related thermal anomaly. The
156 interpretation that this volcanism is associated with a deep-seated mantle plume needs to be
157 reconciled with the long duration of magmatism and the rapid equatorward motion of North
158 America from a latitude of ~54° N *ca.* 1108 Ma during early stage flood basalt eruptions to ~32°
159 N by the *ca.* 1096 Ma main stage (paleolatitudes for the location of Duluth, MN). While some of
160 this motion could be associated with true polar wander, in which the mesosphere and
161 asthenosphere rotated in conjunction with the lithosphere, Swanson-Hysell et al. (2019) showed
162 that the record of paleomagnetic poles requires a substantial component of differential plate
163 tectonic motion. The pulsed nature of magmatic activity could support a model wherein there
164 were multiple upwelling pulses. As postulated by Cannon and Hinze (1992), the initial pulse
165 expressed by *ca.* 1108 early stage flood basalt volcanism initiated lithospheric thinning. Given the
166 significantly thinned lithosphere in the Midcontinent Rift region, subsequent positively-buoyant
167 plume material that encountered Laurentia lithosphere would have experienced “upside-down”
168 drainage wherein relief at the base of the lithosphere resulted in lateral and upward flow into the

169 Midcontinent Rift (Sleep, 1997; Swanson-Hysell et al., 2014). Flow of upwelling mantle to where
170 the lithosphere was locally thin would have led to ponding and concentrated decompression
171 melting within the rift axis region. One scenario is that Laurentia was migrating over a plume
172 generation zone (Burke et al., 2008) from which multiple deep-seated mantle plumes upwelled to
173 the lithosphere over that time interval. The first could have been centered on the present-day
174 Lake Superior region with the second encountering Laurentian lithosphere and being directed to
175 the rift by upside-down drainage in addition to driving magmatism in southwest Laurentia.
176 Another scenario is that *ca.* 1096 Ma magmatism was invigorated by upwelling return flow
177 enhanced by slab avalanche induced downwelling connected to the rapid plate motion of
178 Laurentia that initiated in the early stage (Swanson-Hysell et al., 2019). Overall, the constraint
179 that both the anorthositic and layered series of the Duluth Complex were emplaced in less than 1
180 million years requires an exceptional thermal anomaly that lead to voluminous rapid melt
181 generation during the main stage of Midcontinent Rift development.

182 ACKNOWLEDGEMENTS

183 Project research was supported by NSF EAR-1847277 (awarded to NLS-H) and the University of
184 Minnesota, Duluth. Funding for the analytical infrastructure of the Boise State University Isotope
185 Geology Laboratory was provided by NSF EAR-0824974 and EAR-0521221. Margaret Avery and
186 Dan Costello provided field assistance. Debbie Pierce assisted with analyses at Boise State.

187 References

- 188 Beck, M., 1970, Paleomagnetism of Keweenawan intrusive rocks, Minnesota: Journal of Geophysical Research,
189 vol. 75, pp. 4985–4996, doi:10.1029/JB075i026p04985.
- 190 Blackburn, T. J., Olsen, P. E., Bowring, S. A., McLean, N. M., Kent, D. V., Puffer, J., McHone, G., Rasbury, E. T.,
191 and Et-Touhami, M., 2013, Zircon U-Pb geochronology links the end-Triassic extinction with the Central
192 Atlantic Magmatic Province: Science, vol. 340, pp. 941–945, doi:10.1126/science.1234204.
- 193 Bright, R. M., Amato, J. M., Denyszyn, S. W., and Ernst, R. E., 2014, U-Pb geochronology of 1.1 Ga diabase in the
194 southwestern United States: Testing models for the origin of a post-Grenville large igneous province:
195 Lithosphere, vol. 6, pp. 135–156, doi:10.1130/L335.1.
- 196 Burgess, S. D., Bowring, S. A., Fleming, T. H., and Elliot, D. H., 2015, High-precision geochronology links the
197 Ferrar large igneous province with early-Jurassic ocean anoxia and biotic crisis: Earth and Planetary Science
198 Letters, vol. 415, pp. 90–99, doi:10.1016/j.epsl.2015.01.037.

- 199 Burke, K., Steinberger, B., Torsvik, T. H., and Smethurst, M. A., 2008, Plume generation zones at the margins of
200 large low shear velocity provinces on the core–mantle boundary: *Earth and Planetary Science Letters*, vol. 265,
201 pp. 49–60, doi:10.1016/j.epsl.2007.09.042.
- 202 Cannon, W. F., 1992, The Midcontinent rift in the Lake Superior region with emphasis on its geodynamic
203 evolution: *Tectonophysics*, vol. 213, pp. 41–48, doi:10.1016/0040-1951(92)90250-A.
- 204 Cannon, W. F. and Hinze, W. J., 1992, Speculations on the origin of the North American Midcontinent rift:
205 *Tectonophysics*, vol. 213, pp. 49–55, doi:10.1016/0040-1951(92)90251-Z.
- 206 Condon, D. J., Schoene, B., McLean, N. M., Bowring, S. A., and Parrish, R. R., 2015, Metrology and traceability of
207 U–Pb isotope dilution geochronology (EARTHTIME tracer calibration part I): *Geochimica et Cosmochimica
208 Acta*, vol. 164, pp. 464–480, doi:10.1016/j.gca.2015.05.026.
- 209 Davis, D. and Green, J., 1997, Geochronology of the North American Midcontinent rift in western Lake Superior
210 and implications for its geodynamic evolution: *Canadian Journal of Earth Science*, vol. 34, pp. 476–488,
211 doi:10.1139/e17-039.
- 212 Edwards, G. H. and Blackburn, T., 2018, Detecting the extent of ca. 1.1 Ga Midcontinent Rift plume heating using
213 U–Pb thermochronology of the lower crust: *Geology*, vol. 46, pp. 911–914, doi:10.1130/g45150.1.
- 214 Fairchild, L. M., Swanson-Hysell, N. L., Ramezani, J., Sprain, C. J., and Bowring, S. A., 2017, The end of
215 Midcontinent Rift magmatism and the paleogeography of Laurentia: *Lithosphere*, vol. 9, pp. 117–133,
216 doi:10.1130/L580.1.
- 217 Green, J., 1983, Geologic and geochemical evidence for the nature and development of the Middle Proterozoic
218 (Keweenawan) Midcontinent Rift of North America: *Tectonophysics*, vol. 94, pp. 413–437,
219 doi:10.1016/0040-1951(83)90027-6.
- 220 Green, J. C., Boerboom, T. J., Schmidt, S. T., and Fitz, T. J., 2011, The North Shore Volcanic Group:
221 Mesoproterozoic plateau volcanic rocks of the Midcontinent Rift System in northeastern Minnesota: *GSA Field
222 Guides*, vol. 24, pp. 121–146, doi:10.1130/2011.0024(07).
- 223 Jaffey, A., Flynn, K., Glendenin, L., Bentley, W., and Essling, A., 1971, Precision measurement of half-lives and
224 specific activities of ^{235}U and ^{238}U : *Physical Review*, vol. C4, pp. 1889–1906, doi:10.1103/PhysRevC.4.1889.
- 225 Jirsa, M. A., Boerboom, T., Chandler, V., Mossler, J., Runkel, A., and Setterholm, D., 2011, S-21 Geologic map of
226 Minnesota-bedrock geology: Tech. rep., Minnesota Geological Survey, URL
227 <http://hdl.handle.net/11299/101466>.
- 228 Mattinson, J. M., 2005, Zircon U/Pb chemical abrasion (CA-TIMS) method: Combined annealing and multi-step
229 partial dissolution analysis for improved precision and accuracy of zircon ages: *Chemical Geology*, vol. 220, pp.
230 47–66, doi:10.1016/j.chemgeo.2005.03.011.
- 231 Miller, J., James D., Green, J. C., Severson, M. J., Chandler, V. W., and Peterson, D. M., 2001, M-119 Geologic
232 map of the Duluth Complex and related rocks, northeastern Minnesota: Tech. rep., Minnesota Geological Survey.
- 233 Miller, J., J.D., Green, J., Severson, M., Chandler, V., Hauck, S., Peterson, D., and Wahl, T., 2002, Geology and
234 mineral potential of the Duluth Complex and related rocks of northeastern Minnesota: Minnesota Geological
235 Survey Report of Investigations, vol. 58.
- 236 Nicholson, S. W. and Shirey, S. B., 1990, Midcontinent Rift Volcanism in the Lake Superior Region: Sr, Nd, and Pb
237 Isotopic Evidence for a Mantle Plume Origin: *J. Geophys. Res.*, vol. 95, pp. 10,851–10,868,
238 doi:10.1029/JB095iB07p10851.

- 239 Paces, J. and Miller, J., 1993, Precise U-Pb ages of Duluth Complex and related mafic intrusions, northeastern
240 Minnesota: Geochronological insights to physical, petrogenetic, paleomagnetic and tectonomagmatic processes
241 associated with the 1.1 Ga Midcontinent Rift System: *Journal of Geophysical Research*, vol. 98, pp.
242 13,997–14,013, doi:10.1029/93jb01159.
- 243 Schmitz, M. D., 2012, The Geologic Time Scale, Elsevier, Boston, chap. 6 – Radiogenic Isotope Geochronology, pp.
244 115–126: doi:10.1016/B978-0-444-59425-9.00006-8.
- 245 Schoene, B., Crowley, J. L., Condon, D. J., Schmitz, M. D., and Bowring, S. A., 2006, Reassessing the uranium
246 decay constants for geochronology using ID-TIMS U–Pb data: *Geochimica et Cosmochimica Acta*, vol. 70, pp.
247 426–445, doi:10.1016/j.gca.2005.09.007.
- 248 Schoene, B., Eddy, M. P., Samperton, K. M., Keller, C. B., Keller, G., Adatte, T., and Khadri, S. F. R., 2019, U-Pb
249 constraints on pulsed eruption of the Deccan Traps across the end-Cretaceous mass extinction: *Science*, vol. 363,
250 pp. 862–866, doi:10.1126/science.aau2422.
- 251 Sleep, N. H., 1997, Lateral flow and ponding of starting plume material: *Journal of Geophysical Research: Solid
252 Earth*, vol. 102, pp. 10,001–10,012, doi:10.1029/97JB00551.
- 253 Sprain, C. J., Renne, P. R., Vanderkluysen, L., Pande, K., Self, S., and Mittal, T., 2019, The eruptive tempo of
254 Deccan volcanism in relation to the Cretaceous-Paleogene boundary: *Science*, vol. 363, pp. 866–870,
255 doi:10.1126/science.aav1446.
- 256 Stein, C. A., Kley, J., Stein, S., Hindle, D., and Keller, G. R., 2015, North America’s Midcontinent Rift: When rift
257 met LIP: *Geosphere*, doi:10.1130/GES01183.1.
- 258 Swanson-Hysell, N. L., Ramezani, J., Fairchild, L. M., and Rose, I. R., 2019, Failed rifting and fast drifting:
259 Midcontinent Rift development, Laurentia’s rapid motion and the driver of Grenvillian orogenesis: *GSA Bulletin*,
260 doi:10.1130/b31944.1.
- 261 Swanson-Hysell, N. L., Vaughan, A. A., Mustain, M. R., and Asp, K. E., 2014, Confirmation of progressive plate
262 motion during the Midcontinent Rift’s early magmatic stage from the Osler Volcanic Group, Ontario, Canada:
263 *Geochemistry Geophysics Geosystems*, vol. 15, pp. 2039–2047, doi:10.1002/2013GC005180.
- 264 Tauxe, L., Shaar, R., Jonestrask, L., Swanson-Hysell, N., Minnett, R., Koppers, A., Constable, C., Jarboe, N.,
265 Gaastra, K., and Fairchild, L., 2016, PmagPy: Software package for paleomagnetic data analysis and a bridge to
266 the Magnetics Information Consortium (MagIC) Database: *Geochemistry, Geophysics, Geosystems*,
267 doi:10.1002/2016GC006307.
- 268 Vervoort, J., Wirth, K., Kennedy, B., Sandland, T., and Harpp, K., 2007, The magmatic evolution of the
269 Midcontinent rift: New geochronologic and geochemical evidence from felsic magmatism: *Precambrian Research*,
270 vol. 157, pp. 235–268, doi:10.1016/j.precamres.2007.02.019.
- 271 White, R. and McKenzie, D., 1995, Mantle plumes and flood basalts: *Journal of Geophysical Research: Solid Earth*
272 (1978–2012), vol. 100, pp. 17,543–17,585, doi:10.1029/95JB01585.